Available online at www.sciencedirect.com

ScienceDirect

Procedia Structural Integrity 12 (2018) 567–577

Structural Integrity Procedia

www.elsevier.com/locate/procedia

AIAS 2018 International Conference on Stress Analysis

Combined use of confocal microscopy and DIC for 3D displacement vector measurement

Luigi Bruno*

University of Calabria, DIMEG, Via Bucci 44C, Rende (CS) 87036, Italy

Abstract

In the present paper the author describes the potential offered by the combined use of the Confocal Microscopy (CM) and Digital Image Correlation (DIC) to resolve the whole displacement vector in full-field fashion and with nanometric accuracy. By means of two different configurations of the same portion of the area under investigation, the surface profile retrieved at microscopic level by the CM functioned as a carrier for the DIC algorithm, both for a polished surface and an engineering standard roughness. The in-plane displacement components obtained by DIC were then used to extract the out-of-plane component from the profile information. After describing all steps that are necessary for applying the procedure, preliminary results of an indentation tests carried out on a polished steel specimen are reported and discussed.

Keywords: Digital image correlation; confocal microscopy; dispalcement vector.

1. Introduction

The impressive development of new materials that has been observed in recent last decades, especially in the field of electronics, biomechanics and nanotechnologies, has pushed investigative techniques in the mechanics of materials towards new frontiers and methodologies (Young et al. (2012), Gleiter et al. (2014)). In most cases, what makes these new materials

* Corresponding author. Tel.: +39-0984-494839; fax: +39-0984-494673.
E-mail address: luigi.bruno@unical.it

10.1016/j.prostr.2018.11.062

unique is their microscopic structure, which implies peculiar behavior that cannot be found in conventional materials. Because of this, the corresponding techniques and methodologies must be able to perform measurements at the micro- or even nano-scale with an acceptable accuracy, in order to provide useful information that would allow for the design of new applications using these materials.

By limiting the focus to the mechanical properties, full-field non-contact techniques capable of measuring the displacement field represent an appealing tool that allows for a better understanding of the mechanics of these materials at different scale levels. Among all these techniques (Rastogi (2000)), it is possible to identify two classes that are commonly used to extract mechanical deformation on a 2D (or even a 3D) domain without physical contact with the sample: interferometric techniques and correlation procedures. The former allows for high sensitivity but requires complex experimental setups, especially when more than a single displacement component needs to be retrieved. On the contrary, correlation approaches consist of simpler experimental arrangements that provide significantly lower sensitivity.

Because of their methodological simplicity, in recent years DIC methods have seen a wide and quick diffusion, both in academic and industrial areas. Today different shareware (Ncorr) and commercial software (Correlated Solutions) are available, and even a non-expert photo-mechanics end-user can easily carry out simple DIC analyses. Nevertheless, the aforementioned low sensitivity of this type of method still represents the most present challenge for DIC users. Its capability to comprehend how close the performed measurements are to an acceptable accuracy threshold is what makes this experimental investigation tool reliable.

With the aim of enhancing the accuracy of DIC methods, innovative measurement approaches were proposed: their common feature is the ability to improve the resolution of images to which the correlation algorithms are applied. Among the different means to such an end explored by the researchers, the followings were of note. High resolution scanning methods, such as Scanning Electron Microscopy – SEM – (Stinville et al. (2016)), Transmission Electron Microscopy – TEM – (Wang et al. (2015)) and Electron Back-Scatter Diffraction – EBSD – (Jiang et al. (2016)), allowed for a resolution of details on the samples under investigation at a level not possible to achieve by way of a conventional imaging medium, such as a system formed by a CCD camera and a lens. This approach significantly improved the resolution on the evaluation of in-plane displacement components, but it was not capable of providing any information about the out-of-plane component and it easily suffers from defocusing issues. The out-of-plane component can be measured if the high-resolution image of the sample is created by equipment capable of retrieving the profile information, such as Atomic Force Microscopy – AFM – (Han et al. (2010)) or Confocal Microscopy – CM – (van Beeck et al. (2014)). Using these methods, the author demonstrated how to attain high sensitivity on all three displacement components by means of DIC algorithms. Nevertheless, the noise level implied by their applications required specific assumptions on the displacement fields or tailored correlation algorithms (Baldi and Bertolino (2016)) in order to obtain meaningful measurements on the domains under investigation.

In the present study, the author demonstrates in which conditions it is possible to combine CM and DIC to retrieve the whole displacement vector with nanometric accuracy on a portion of the outer surface of a sample. The basic steps of the proposed method are described in details, and it was applied to a real case as an example of how this approach could provide useful information in the field of the mechanics of materials.

2. Materials and methods

The correlation methods used for displacement quantification based on image processing require that the analyzed images have a random texture, which can be identified in two or more different loading configurations through proper correlation algorithms. This texture, sometimes

called “speckles,” should not be confused with the interferometric phenomenon that occurs when a rough surface is illuminated by a coherent light source (Bruno and Poggialini (2016)). The “speckles” texture referred to here is normally obtained through the proper application of paint to the area of the studied sample. Less often, a surface treatment can be carried out, such as a sandblast or manual texturing with sand paper. In some particular optical configurations, such as those for a high magnification ratio, it is even possible to use the surface as it is. In all these operating conditions, the resolution of DIC methods on the displacement components depends on the physical size of the pixel and the optical performance of the lens used to focus the objects on the camera sensor. By neglecting lens distortion, depending on the effectiveness of the correlation algorithm, the resolution will range from 1 up to 1/100 of the pixel’s physical size. In conclusion, in most conditions, taking into consideration the size and dimensions of the actual camera sensors, it is hard to reach resolutions under 0.5 μm on the displacement. In addition, this optimal accuracy can be obtained only through a conventional DIC approach, which requires the observation of a flat surface along its normal and which is capable of measuring only the two in-plane components.

On the other hand, if the surface image is sampled by a profilometer, the smallest detail – i.e. the distance between the two closest points – can be significantly smaller than that obtained by an image acquired optically by a lens. Figure 1a shows the profile of a 40 μm x 40 μm portion of the area sampled using the 200 x 200 points acquired by an optical profilometer. The same profile can be represented as a 2D image, as depicted in Fig. 1b, where the intensity of every “virtual” pixel is proportional to the profile height measured at each point. The adjective “virtual” is used because the pixel is not a real picture element, but a representation of the local height. In this example it is possible to see that the virtual pixel size of the image shown in Fig. 1b is 0.2 μm, which is roughly 1/25 of the typical pixel size (~ 5 μm) of a camera sensor used for DIC experiments. This ratio of about 1/25 is even smaller if we consider the fact that the magnification ratio normally used in DIC experiments is less than 1 – i.e. the analyzed areas are usually bigger than the sensor size.

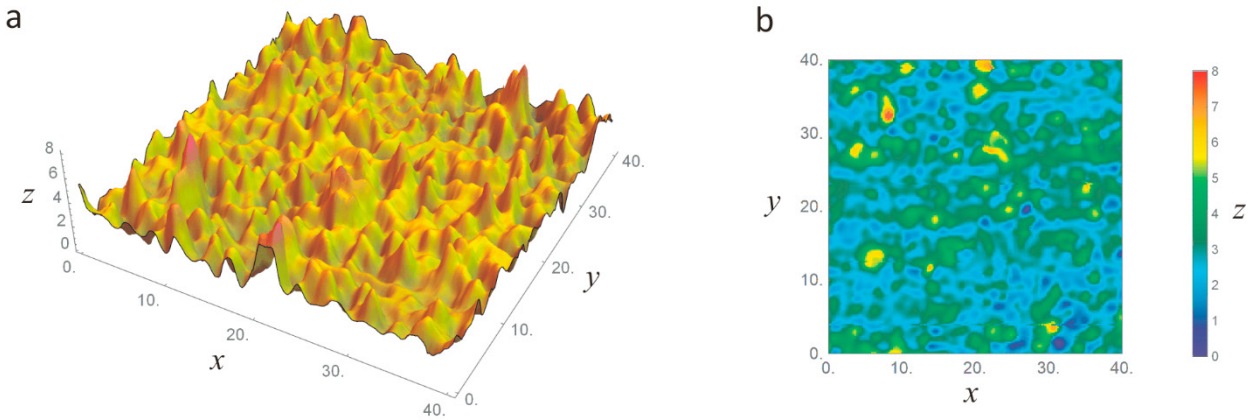

Fig. 1. Surface profile of a 40 μm x 40 μm area sampled by 200 x 200 acquisitions: (a) 3D view; (b) 2D representation. All the axes’ dimensions are in micrometers.

Therefore, the first step of the proposed method consists of applying a standard two-dimensional DIC algorithm to images obtained by profiles acquired through two (or more) different loading configurations. This allows for the evaluation of the two in-plane components with a resolution quantifiable according to the aforementioned remarks. In order to apply the DIC procedures, pixel intensities in the image (obtained from the profile heights) can be remapped in

an 8-bit gray-level scale. This will significantly speed up the convergence of the correlation algorithms, which are normally optimized for 8-bit depth images. To be accurate, beyond the in-plane components, this first analysis step will provide the two displacement components occurring in the plane orthogonal to the axis along which the profile is measured. It is the plane that essentially always coincides with the normal of the surface.

In the next step, the out-of-plane component is retrieved using the profile information from different loading configurations and in-plane components obtained in the first step. In fact, displacement along the normal direction can be evaluated as the height variation of the profile at each point, which is identified by the correlation algorithm in all analyzed loading configurations. Hence, if $z_1(x_1,y_1)$ and $z_2(x_2,y_2)$ are the heights in two different loading configurations at the generic point identified by the coordinates (x_1,y_1) and (x_2,y_2) in the reference systems fixed on the specimen in the two aforementioned configurations, $u_x(x_1,y_1)$ and $u_y(x_1,y_1)$, the in-plane displacement components obtained by the DIC algorithms in the first step, the out-of-plane component $u_z(x_1,y_1)$ can be evaluated as:

$$u_z(x_1, y_1) = z_2\big[x_1 + u_x(x_1, y_1), y_1 + u_y(x_1, y_1)\big] - z_1(x_1, y_1). \tag{1}$$

The operation expressed by eq. (1) can be applied on the experimental data $z_i(x_i,y_i)$ only after they are properly interpolated, which is not necessary given that the in-plane components evaluated by DIC methods are integer number. This will also allow for the calculation of u_z at any point (x,y), not only in correspondence of those points where the profile is measured.

The profilometer used to apply the proposed method is the confocal microscope that an Anton Paar micro- and nano-indentation station (Fig. 2a) is equipped with. The working principle is briefly explained in Fig. 2b. All the wavelengths of a wide spectrum white light source (WLS) are scattered by a dispersive lens (DL). The specific wavelength reflected by the surface of the specimen (SP), according to its height along the z direction, is identified by the spectrometer (SM), which gathers light through a pinhole (PH). A beamsplitter (BS) creates a contemporary perpendicular illumination and allows for the orientation of the spectrometer. The sample profile is retrieved in the xy plane by a two-degrees-of-freedom piezoelectric actuated moving stage, where it is possible to set the length and the number of points to be scanned for each direction. Other operating parameters can be set during the profile acquisition, such as the scanning frequency and path, or the data averaging. The z resolution of this machine is 10 nm, on a total measuring range of 400 μm.

The DIC software used for analyzing the images produced by the profilometer is the VIC-2D (version 2009) distributed by the Correlated Solutions, Inc. The main parameters that require definition in the analyses are the subset and the step size. Using the subset, the operator defines the dimension of the area that should be recognizable through the correlation procedure undertaken in the different loading configurations. It must be large enough to include a sufficient number of details, which are required to obtain a convergence of the correlation algorithm for most of the analyzed subsets. On the other hand, the subset dimension should be kept as small as possible in order to minimize the unavoidable averaging operation on the local gradients of the displacement field. The step size is a less critical parameter, as it defines how to sample the single analyzed image. It mostly impacts the calculation time, and the value chosen should not be much smaller than the subset in order to avoid an oversampling of information that can be extracted from the DIC analyses. Some additional settings can be selected before running the procedure, and a few pre- and post-processing options are made available by the software. For further detail, on-line and on-request manuals can be provided by the vendor (Correlated Solutions), although it is worth noting that the method as presented does not require particularly complex correlation procedures, which means that any DIC software should work properly.

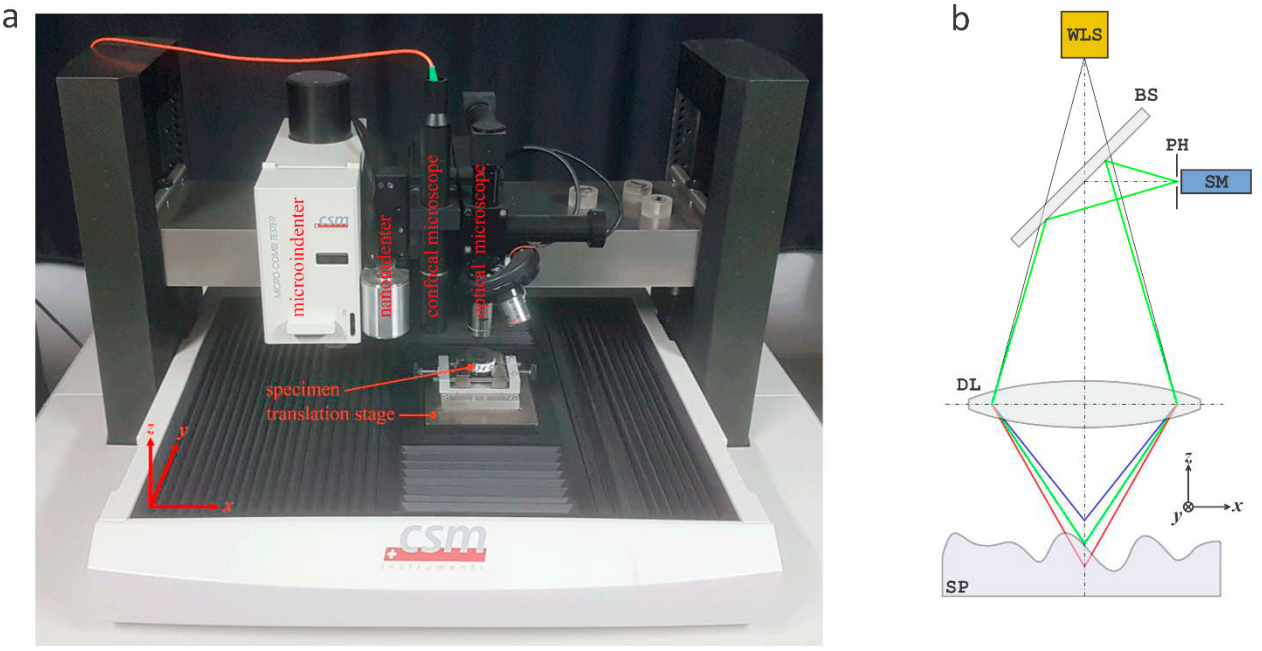

Fig. 2. Experimental setup for profile measurement: (a) micro- and nano-indentation station formed by a microindenter, a nanoindenter, the confocal microscope and the optical microscope; (b) working principle of the confocal microscope (WLS – white light source, BS – beamsplitter, PH – pinhole, SM – spectrometer, DL – dispersive lens, SP – specimen).

3. Results and discussion

The method was initially verified on two surface types in order to test the capability of the correlation algorithm to work in the presence of substantially different levels of roughness. In particular, two dissimilar operating conditions were considered: a conventional roughness usually employed for mechanical parts (Fig. 3a) and a polished surface obtained through standard treatments, normally used to prepare samples for metallographic analyses (Fig. 3b). For both cases, Figure 3 shows a 2D map of the profile in a gray-level representation, the profile of the horizontal centerline (dashed red line) of the 2D map, and a table with the roughness parameters (R_a, average roughness; R_q, root mean square roughness; R_v, maximum height; R_p, maximum depth). In some engineering applications, roughness higher than the case reported in Fig. 3a is certainly possible. Nevertheless, the higher the roughness the less stringent the convergence conditions are for the DIC procedures.

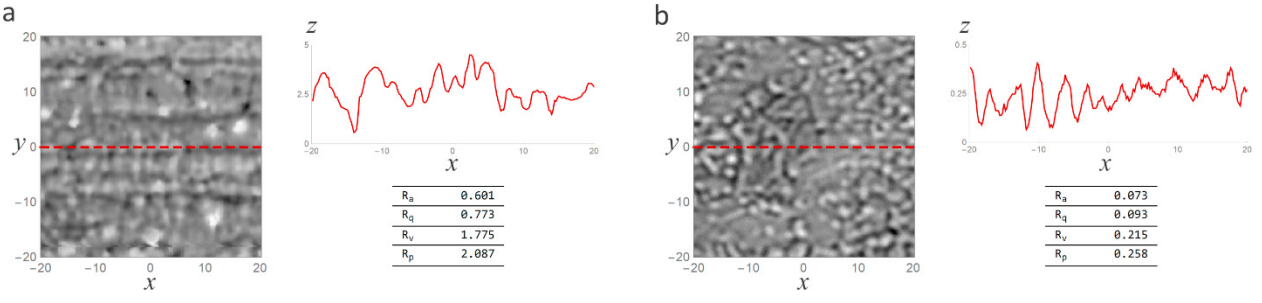

Fig. 3. Two-dimensional map of the profile, profile of the centerline and roughness parameters parameters (R_a, average roughness; R_q, root mean square roughness; R_v, maximum height; R_p, maximum depth) for two different type of surface: a) metal surface finished for engineering parts; b) polished metal surface metallographic analyses. The axes' dimensions and the roughness parameters are in micrometers.

These two surfaces were used to analyze the effect of the subset size on the convergence of the DIC algorithm. The parameter used to evaluate the success of the analysis is the correlation coefficient σ, calculated at each point by the DIC algorithm. If it falls in the range [0,0.1] the convergence is met, otherwise the algorithm assumes, at that point, that the analysis failed and it assigns to σ the value -1. For each analysis, two sample configurations were acquired and no load was applied between them. This "zero test" quantifies the capability of the DIC algorithm to correlate two different configurations in the best operating conditions – i.e. no deformation occurring on the surface under investigation.

The subset size was gradually increased, starting from 9 (minimum value that can be set in the software) and continuing up to the value, over which there is no significant improvement in terms of the amount of useful information retrieved by the DIC algorithm. For this parameter, only odd numbers can be chosen, in order to have a square domain centered on the analyzed pixel. Specifically, in the output report generated after each analysis, the percentage of points with a correlation coefficient different from -1 were counted and plotted on a graph. Figures 4a and 4b show this graph for the two surface types whose properties are reported in the tables of Fig. 3. For the surface with higher roughness (Fig. 4a), the algorithm starts working for a subset size equal to 15, which provides 45% of the successful points, while in order to achieve 95% success it is necessary to raise the size of the subset to 25. On the other hand, for the smoother surface (Fig. 4b), the algorithm starts working for a 13 subset size (33% of success), but it reaches 97% of the success for a 23 subset size. After all, although a magnitude order of difference in terms of roughness, the DIC algorithm works quite similarly on the two surface types, and the maximum value of the subset size required for accurately performing the analysis is small enough to work in the presence of severe working conditions – i.e. high deformation gradients. This procedure is useful when selecting the optimal size of the subset as a function of the morphological feature of the surface under investigation.

Figures 4c and 4d show the spatial distribution of the correlation coefficient σ on a portion of the two surface types considered in the present study. In both cases, the extension of this area is 160 μm x 160 μm, and the subset size was fixed at 25 pixels. It is possible to notice the small number of points where σ is equal to -1 (red dots), which indicates that the DIC algorithm works quite well. As predicted by the graphs in Figs. 4a and 4b, it can also be qualitatively noted that a subset size of 25 pixels provides better results for the smoother surface (R_a = 0.073 μm).

Subsequently, the method was applied to retrieve the displacement vector on a sample subjected to an indentation test. The sample is an AISI 1040 steel block cylindrically shaped (15 mm diameter, 20 mm thickness) hot mounted in thermoplastic resin and polished according to the protocol of a Struers grinding machine. The indentation test was performed by a mechanical hardness machine, applying a load of 2 kg with a 1 mm diameter hardened steel ball. The test consists of three steps. Initially, the profile is acquired by a confocal microscope with the specimen fixed on the micro- and nano-indentation station, as shown in Fig. 2a. At the end of the scanning operation, the specimen is moved under the mechanical hardness machine, and the spherical indentation is applied with attention paid in order to apply this to indent within the same area of the profile previously acquired. In order to mark the area of the specimen whose profile must be retrieved before and after the application of the indentation, a scratch was made on the specimen by manually applying a small amount of pressure with a Phillips screwdriver. The final step consists in re-measuring the profile of the area around the indentation, after manually repositioning the sample under the profilometer.

The mechanical hardness machine is shown in Fig. 5a, where the main parts are properly emphasized: the specimen laying on the vertical translation stage and the machine head where, with the adjustment of a mechanical lever, both an optical microscope and the mount of the indenter can be accessed.

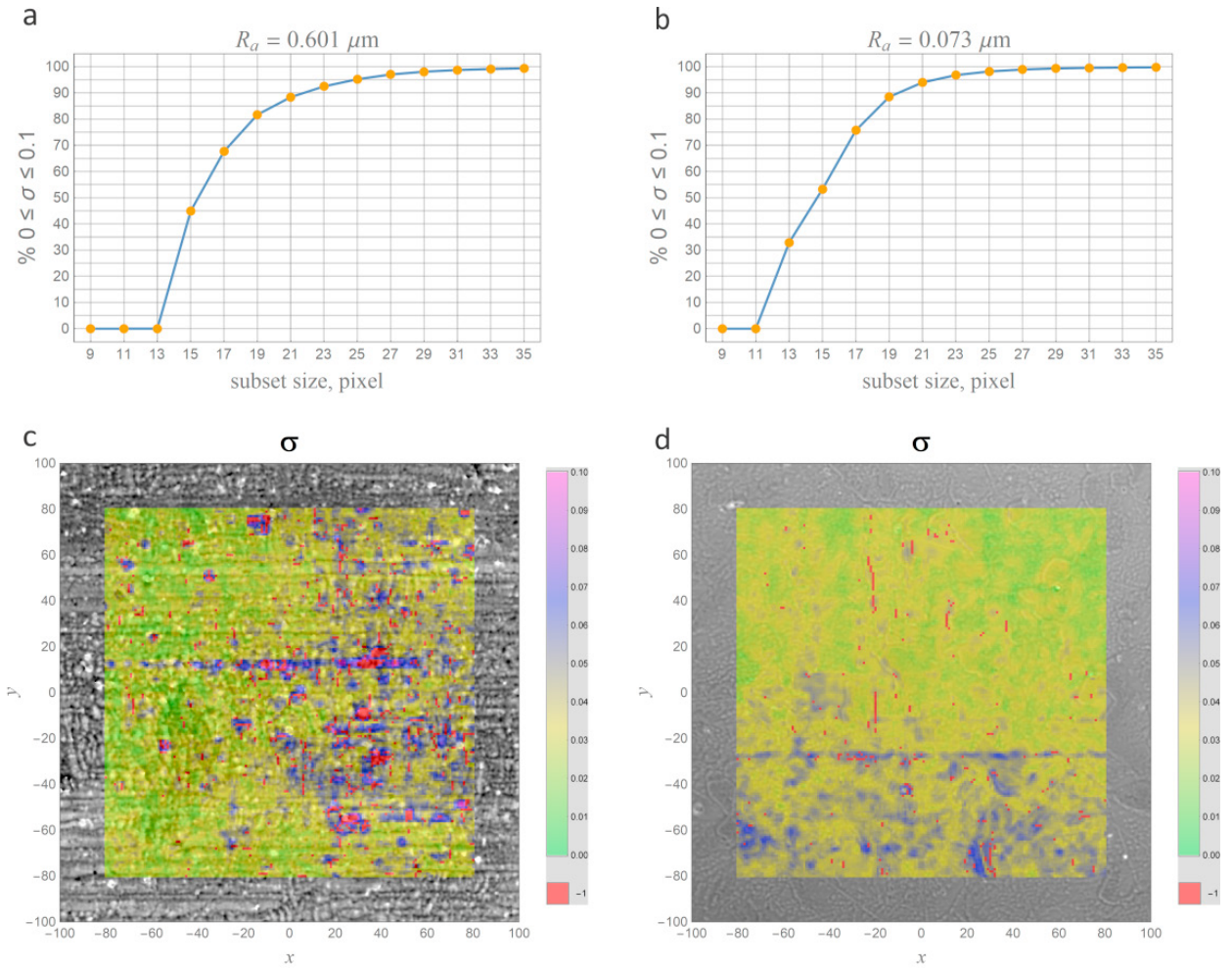

Fig. 4. Results of the procedure for selecting the subset size: a) correlation coefficient versus subset size for the surface with a roughness typical for many engineering applications (R_a = 0.601 μm); b) correlation coefficient versus subset size for the polished surface (R_a = 0.073 μm); correlation coefficient maps obtained for a subset size equal to 25 pixel calculated c) on the rougher surface and d) on the smoother surface. The *xy* axes' dimensions are in micrometers, the correlation coefficient is non-dimensional.

The profile of the specimen was sampled before and after the application of the indentation, at 2000 pixels x 2000 pixels uniformly distributed over an area of 400 μm x 400 μm. Again, the pixel step was set to 0.2 μm. Figure 5b shows the correlation coefficient distribution over the region of interest on the specimen, defined as 300 μm x 300 μm. A length of 100 μm was lost along both the *x* and *y* directions, due to the error caused while repositioning the specimen between the two profile acquisitions, which was performed manually after the indentation application. According to the selection procedure discussed above, the subset size was set to 25 pixels. It is apparent that the points falling inside the indentation area do not carry any displacement information, due to the high plastic deformation occurring in this region, which inevitably destroys the carrier for the DIC algorithm. On the other hand, it is worth noting that the points that do not provide useful deformation measurements (σ = -1, red dots) are relatively few in number if the indentation area is excluded. They represent merely 5.4% of the total.

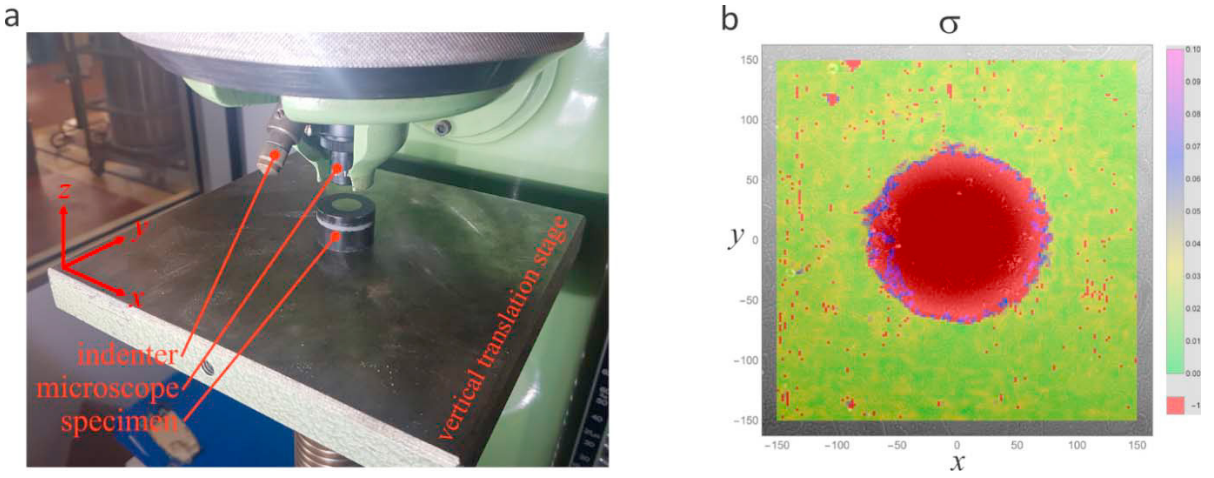

Fig. 5. The experiment carried out on a hot-mounted AISI 1040 steel specimen: a) the mechanical hardness machine; b) spatial distribution of the correlation coefficient σ. The axes' dimensions are in micrometers, correlation coefficient is non-dimensional.

Finally, the experimental results obtained on the indented specimen are shown in Fig. 6. In particular, the profile maps generated before and after the execution of the indentation are shown in Figs. 6a and 6b, respectively. The maps are represented in a gray-level density plot, but the scale is not reported because the plot range was adjusted in order to better emphasize the correlating part of the surface between the two images. In the non-deformed configuration (Fig. 6a), the scratch made manually to identify the indentation area is clearly visible. The three displacement components u_x, u_y and u_z retrieved by the proposed method are shown in Figs. 6c, 6e, and 6g, respectively, while each is represented by a density plot whose color scale was properly set according to the range that corresponds to each component. The plot was superimposed as a colored layer on the deformed profile map in order to associate each point with its own displacement component.

Subsequently, each component was fitted according to the procedure proposed in Bruno (2016), according to which a set of piecewise B-spline functions were defined in the region of interest and weighted after a least mean square optimization process, which does not require any iteration. The fitted displacement components are shown in Figs. 6d, 6f, and 6h, where they are represented by a contour plot using the same color range as the corresponding raw data density plot.

It is worth noting how the range differs between the in-plane and out-of-plane components: whereas the in-plane components span a range of 13-24 micrometers, the out-of-pane component, in the same region of interest, spans a range of just 1 micrometer. This result is expected for a deformation field developed around an indentation obtained by a spherical ball, and it demonstrates how the proposed method can serve as a useful investigation tool, offering a deeper understanding of mechanics than conventional methods commonly used for this type of case studies.

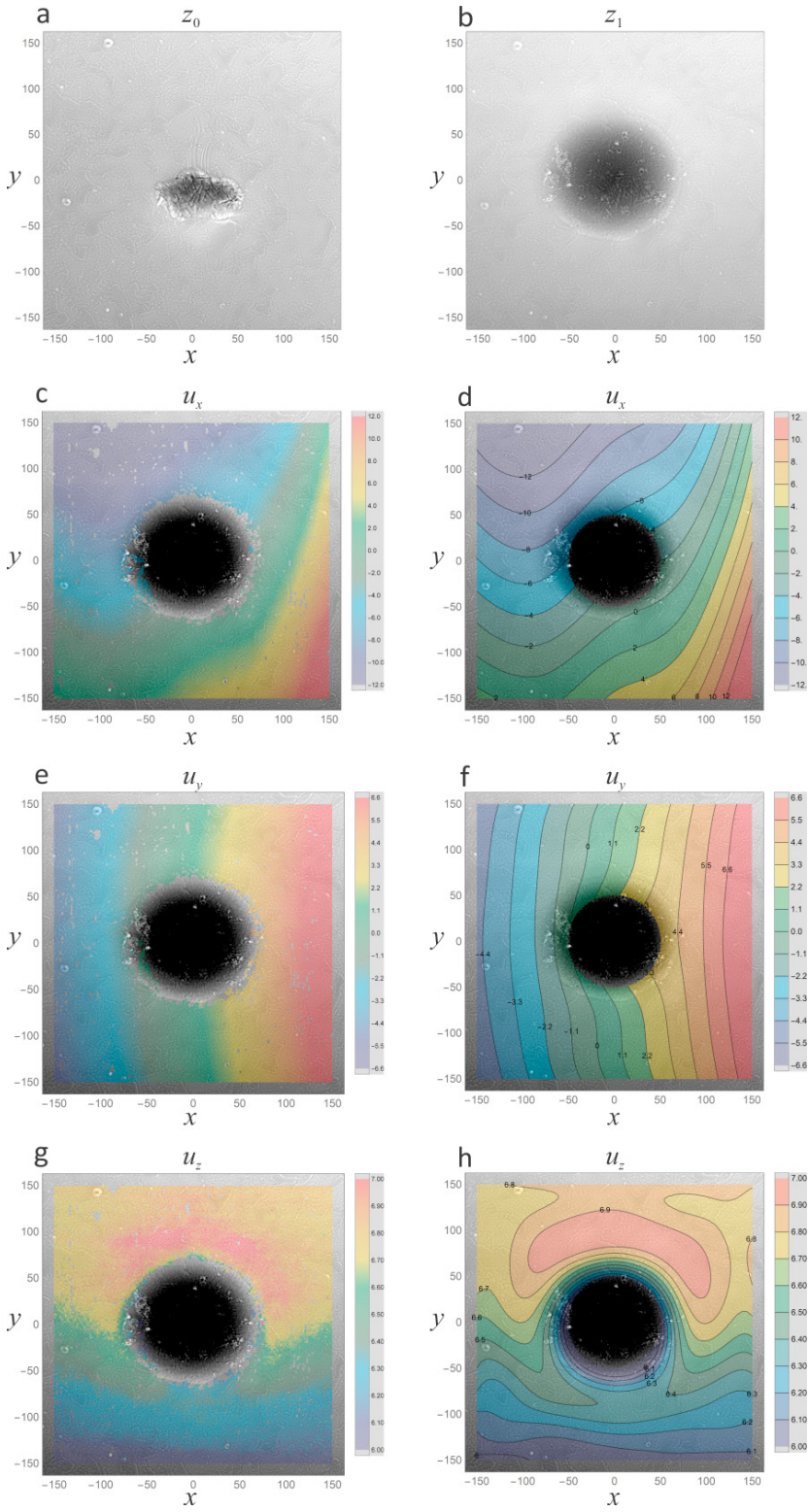

Fig. 6. Experimental results: a) profile before indentation; b) profile after indentation; c) u_x before fitting; d) u_x after fitting; e) u_y before fitting; f) u_y after fitting; g) u_z before fitting; h) u_z after fitting. The axes' dimensions and displacement bars are in micrometers.

The resolution obtained on the displacement vector measurements can be estimated by making some considerations about the DIC method applied and the equipment used for retrieving the surface profile. In particular, because the method consists of two steps, the first for the in-plane and the second for the out-of-plane measurement, it is reasonable to attain two different resolutions for the two different types of displacement components. The commercial DIC software vendors, like the one used in the present application, normally claim up to 1/100 pixel resolution when the measurements are carried out in optimal conditions. This is a quite optimistic estimation of the accuracy level attainable by the application of DIC methods, but it is certainly more than reasonable to diminish this limit by a factor of 5. Hence, assuming a resolution on the in-plane components of 1/20 pixel would not be overestimating the method, as it can be even higher in situations where profiles are retrieved with low levels of noise. Consequently, by considering the dimension of the pixel (0.2 μm), it is possible to conclude that the accuracy on the in-plane components is equal to 10 nm. With regards to the out-of-plane resolution, it depends on the profile accuracy and capability of the DIC algorithm to locate the point in the different loading configurations. By assuming the previous resolution on the in-plane components (1/20 pixel), it is possible, in first approximation, to neglect the location error. Therefore, the out-of-plane resolution coincides with that of the profilometer, which is, according to vendor data sheet, equal to 10 nm.

The fact that the resolution of the two types of displacement components resulted the same is merely a coincidence. In fact, the resolution of the profilometer used in the present study is not extraordinary, given that it is not a specialized machine, but is instead part of a measurement station thus designed for the needs of other machines with which the station is equipped. Actually, it is not difficult to find a commercial profilometer with a resolution lower than 1 nanometer. Moreover, the in-plane resolution can be improved by sampling the profile more finely, but in this case it is necessary to take into account both the spot maximum size (non-contact optical profilometer) or the tip radius of the stylus (contact mechanical profilometer), and the actual spatial frequency of the profile. In some cases, indeed, an oversampling of the profile will not add significant details to allow for the generation of the random structure necessary to make the DIC algorithm work properly.

4. Conclusions

The author proposes a full-field method to measure the displacement vector on a portion of the outer surface of a sample with nanometric accuracy. The experimental data required to apply the method are minimal: two surface profiles, acquired by any type of profilometer, in two or more loading configurations. The comparison between different configurations is carried out by DIC methods, which will retrieve the in-plane components. Subsequently, these are used to extract the out-of-plane component by exploiting the profile information. The method was proven in the present study through the use of a confocal microscope, whose profile data were analyzed with commercial DIC software. The post-processing operations were performed through simple custom routines, implemented using Wolfram Mathematica, that is capable of standard image-processing and list manipulation operations. The resolution achieved in the present study was 10 nm for each displacement component, although a better resolution could be attained using different experimental equipment, i.e. a higher sensitivity profilometer.

The main strengths of the proposed method include its high sensitivity, straightforwardness, and ability to be easily embedded in hardware control software. Apart from the aforementioned high levels of sensitivity, the only data set required by the method is a single profile distribution from each loading configuration to be analyzed. By comparing these configurations, all three displacement components can be extracted, a fact that offers a considerable advantage when compared with interferometric techniques, which are generally capable of measuring one component at a time, or with a standard two-dimensional DIC method, which can extract only

two components per analysis. In addition, due to the fact only standard software tools were used – i.e. commercial DIC software and conventional post-processing operations – the method is easily implement within the management software of a profilometer, with the aim of providing end users with an addition analysis tool.

On the other hand, some weaknesses could arise during the use of this method. If the profilometer is based on a scanning operation, such as the one used in this study, the errors occurring from this operation will bias the in-plane components, although they will not have any impact on the out-of-plane component. In addition, this way of acquiring data does not work for a time-dependent application, unless the acquisition speed is significantly higher than the phenomenon evolution. Another concern could arise from the shape of the surface under investigation. If it is not planar, the profilometer will measure not only the deviation from a plane due to the roughness asperities, but also the macro-geometrical features of the specimen. This is not a limitation of the method, but it could easily become a limitation of the profilometer, which is designed with a limited measurement range, such as a few hundreds of micrometers, which is bigger than any possible roughness level that would occur in engineering applications. Finally, as shown by the experiment carried out on the indented surface, an overly high level of plastic deformation on the outer surface causes carrier deterioration. Hence, if the plastic phenomena occur on a significant portion of the region of interest, the DIC algorithm will fail on the majority of the analyzed points and, therefore, the overall result of the method will be quite poor.

The proposed method can be successfully applied in several fields. All samples characterized by a minimum surface roughness (even a few dozen nanometers, as shown in Fig. 3b) whose mechanics are characterized by nano- and micro-displacement field can be advantageously studied through this approach, despite the complexity of their shape and deformation distribution, such as some fracture mechanics problems occurring at a lower scale than that normally analyzed by standard approaches. The displacement field occurring around nano- and micro-indentations used for the mechanical characterization of coating, advanced ceramics and metallic alloys can be profitably retrieved as well. Residual stress problems, based on displacement relief around blind hole, annular cave or linear scratch represent other case studies that could be potentially addressed by such a method.

References

Baldi, A., Bertolino, F., 2016. Assessment of h-refinement procedure for global digital image correlation. Meccanica 51, 979–991.

Bruno, L., Poggialini A., 2007. Back to the future: from speckle to holography. Optics and Lasers in Engineering 45, 538–549.

Bruno, L., 2016. Isoparametric fitting: a method for approximating full-field experimental data distributed on any shaped 3D domain, Optics and Lasers in Engineering 87, 185–190.

Correlated Solutions, 2018. Correlated Solutions website. URL: http://correlatedsolutions.com/vic-2d/. Last retrieved in date 2018-09-01.

Gleiter, H., Schimmel, T., Hahn, H., 2014. Nanostructured solids - From nano-glasses to quantum transistors. Nano Today 9, 17–68.

Han, K., Ciccotti, M., Roux, S., 2010. Measuring nanoscale stress intensity factors with an atomic force microscope, Europhysics Letters 89, 66003.

Jiang, J., Yang, J., Zhang, T., Zou, J., Wang, Y., Dunne, F.P.E., Britton, T.B., 2016. Microstructurally sensitive crack nucleation around inclusions in powder metallurgy nickel-based superalloys. Acta Materialia 117, 333–344.

Ncorr, 2018. Ncorr website. URL: http://www.ncorr.com/index.php/. Last retrieved in date 2018-09-01.

Rastogi, P.K. (Ed.), 2000. Photomechanics. Springer-Verlag, Berlin Heidelberg.

Stinville, J.C., Echlin, M.P., Texier, D., Bridier, F., Bocher, P., Pollock, T.M., 2016. Sub-grain scale digital image correlation by electron microscopy for polycrystalline materials during elastic and plastic deformation. Experimental Mechanics 56, 197–216.

van Beeck, J., Neggers, J., Schreurs, P.J.G., Hoefnagels, J.P.M., Geers, M.G.D., 2014. Quantification of three-dimensional surface deformation using global digital image correlation. Experimental Mechanics 54, 557–570.

Wang, X., Pan, Z., Fan, F., Wang, J., Liu, Y., Mao, S.X., Zhu, T., Xia, S., 2015. Nanoscale deformation analysis with high-resolution transmission electron microscopy and digital image correlation. Journal of Applied Mechanics, Transections ASME 82, 121001.

Young, R.J., Kinloch, I.A., Gong, L., Novoselov, K.S., 2012. The mechanics of graphene nanocomposites: A review. Composites Science and Technology 72, 1459–1476.